JOURNAL OF PURE AND APPLIED MICROBIOLOGY, April 2013. Vol. **7**(Spl. Edn.), p. 357-367

Morphology Variability Analysis of Wrist Pulse Signal Based on Multiscale Entropy and Recurrence Quantification Analysis

Yan Jianjun[1]*, Wang Yiqin[2]*, Guo Rui[2], Yan Haixia[2] and Zhou Chiheng[1]

[1]Center for Mechatronics Engineering, East China University of Science and Technology, Shanghai - 200 237, P. R. China.
[2]TCM Syndrome Lab, Shanghai University of Traditional Chinese Medicine, Shanghai - 201 203, P. R. China.

(Received: 03 March 2013; accepted: 14 April 2013)

The wrist pulse has been used to diagnose diseases for thousands of years in Traditional Chinese Medicine (TCM). It can reflect the condition of the cardiovascular system, which involves a great deal of nonlinearity. The traditional linear analysis may exclude the nonlinear properties of wrist pulse signals, and the interval variability analysis of pulse signals may be inadequate when changes in pulse morphology are not considered. Therefore, windowed multiscale entropy (WMSE) are proposed and windowed recurrence quantification analysis (WRQA) are used, both of which consider the effect of changes in the morphology of a pulse signal, in the current paper to analyze three TCM pulse signals, namely, normal, slippery, and wiry pulses. The results from the current study reveal clearly that when the cardiovascular system is represented by a wiry pulse, there is a loss of complexity in the results of WMSE and WRQA compared with the results from other kinds of pulse signals. Although the differences in the analyzed results between the normal and slippery pulse signals are not as significant as those between the wiry pulse signals and the two other groups, normal pulse signals are found to be slightly more stable than slippery signals based on SWMSE and SWRQA. The classification results show that these analyses are useful in distinguishing the three common kinds of TCM pulses to benefit pulse diagnosis. The analysis of pulse signals using WMSE and WRQA, both of which consider the effect of changes in the morphology of a pulse signal, is appropriate and may be useful for distinguishing the three common kinds of pulses defined in TCM, thereby benefitting pulse diagnosis.

Key words: Pulse diagnosis, Morphology variability analysis, Multiscale entropy, Recurrence quantification analysis, Traditional Chinese Medicine.

Wri[1]st pulse diagnosis has been used to diagnose diseases for thousands of years in TCM. With the help of modern medicine techniques, the mechanisms for the generation of human pulses and the amount of important information pulse signals contain can be determined easily, and these can reflect the condition of the body (Crilly *et al*.,2007), especially that of the cardiovascular system.

* To whom all correspondence should be addressed.
E-mail: jjyan@ecust.edu.cn (Yan Jianjun),
wangyiqin2380@sina.com (Wang Yiqin)

In traditional pulse diagnosis, the beating of the pulse is felt at the measuring position of the radial artery through the fingertips of a practitioner, which means that the diagnosis depends heavily on the practitioner's skills and experience. To eliminate subjectivity in pulse diagnosis, which is not acceptable to many people, the development of computerized pulse signal analysis methods is necessary to standardize and objectify pulse diagnosis.

Many studies have used a number of methods for pulse signal analysis such as time domain, frequency domain, and time-frequency

domain analyses of pulse signals (Qian, 1994; Fei, 1991; Chen *et al*.,2009; Wu *et al*., 2008; Lee *et al*., 1983; Song *et al*., 1997; Wang *et al*., 2001; Xie *et al*., 2003; Zhang *et al*., 2008). However, these studies have all been based on the linear theory.

The cardiovascular system is a very complex system. In recent years, with the development of nonlinear dynamics, a large body of evidence has shown that the cardiovascular system involves theoretically a great deal of nonlinearity. Therefore, the pulse signal, as the output of this system, might not be analyzed accurately using only the linear theory. This is because such theory excludes the nonlinear properties of the cardiovascular system. Some studies have already used nonlinear methods such as arterial blood pressure (ABP), echocardiogram (ECG), and heart rate variability (HRV) to analyze biological signals.

Wagner *et al*. examined chaos in blood pressure control. Their studies indicated that the chaos theory is useful in characterizing the regularity and complexity of blood pressure control (Wagner *et al*., 1998). Casaleggio *et al*. investigated ECG signals based on the estimation of Lyapunov exponents using a Jacobian-based method (Casaleggio *et al*., 1997). The characteristics of heart rate variability were quantified using nonlinear analysis methods (Jokinen *et al*., 2001; Chesnokov, 2008; Perakakis *et al*., 2009; Peña *et al*., 2009). Most nonlinear methods based on the chaos theory require a long time series and are highly dimensional. Other methods for measuring complexity based on entropy, such as approximate entropy, sample entropy, multiscale entropy, and entropy measures based on symbolic dynamics, have been proposed to overcome the difficulties in using a nonlinear method. This is especially because a long time series cannot always be obtained conveniently in a clinic.

Costa *et al*. proposed the multiscale entropy method and applied it to the ECG signals of healthy subjects who have congestive heart failure, life-threatening conditions, or atrial fibrillation (Costa *et al*., 2005). Some applications of the methods based on symbolic dynamics proved to be appropriate and efficient in measuring complexity in biological signals (Javorka *et al*., 2008; Bär *et al*., 2009; Wessel *et al*.,2000).

On the other hand, most methods based on symbolic dynamics use signals that select only one particular point of a period from the original time series, such as the R-R interbeat of ECG and HRV signals, for analysis. These signals may be suitable for other types of analysis. However, for wrist pulse diagnosis, they may be insufficient because of the exclusion of the changes in pulse morphology in a single period.

In Ref. (Xu *et al*. 2010), the results between pulse interval variability analysis and pulse morphology variability analysis were compared by approximate entropy using 30 pulse signals taken from normal subjects and another 30 taken from patients suffering from coronary arteriosclerosis disorders. Pulse morphology variability is found to be more efficient than pulse interval variability in assessing the conditions of the human coronary artery. However, in the ref. (Xu *et al*. 2010), it didn't analyze the pulse signals defined by TCM in its true sense, such as normal and wiry pulses, but the signals taken from the healthy people or the patients suffering from one kind of disease defined by Western medicine.

In the current paper, three common kinds of TCM pulse signals, namely, normal, slippery, and wiry pulses are analyzed using windowed multiscale entropy (WMSE), and windowed recurrence quantification analysis (WRQA) is also used, to detect the changes in pulse morphology. The present work aims to find some useful features to distinguish the three kinds of pulse signals with considering the effect of changes in the morphology of a pulse signal. These signals are common in pulse diagnosis in TCM, and indicate the different condition of the cardiovascular system (The detail will describe in Section4). It is expected that analysis of them can help to distinguish these three TCM pulses, thereby benefitting pulse diagnosis.

The current paper is organized as follows. The material and methods are described in Section 2. The analysis and results are presented in Section 3. The discussion is given in Section 4. Finally, the conclusion is presented in Section 6.

MATERIALS AND METHODS

All the samples were supplied by the Center for TCM Information Science and Technology of the Shanghai University of TCM.

These samples were collected at the position of "cun" on the wrists of the patients from the outpatient department of the Subsidiary Hospital of the Shanghai University of TCM. The pulse signals of all subjects are acquired for 60 seconds at the sampling rate of 720Hz. The collected wrist pulse signals included 48 normal pulses, 48 slippery pulses, and 48 wiry pulses, which were all obtained from unhealthy people, except for the normal pulse.

Pulse waveform preprocessing

A baseline drift would inevitably occur in a pulse waveform because of respiration of the subject and motion artifacts. Sometimes, some kinds of drifts will be introduced to the pulse signal by the equipment used for signal collection. The baseline drift must be removed so that the results of the analysis will not be affected. In the current paper, a wavelet transform will be used to remove the baseline drift. A discrete Meyer wavelet is used as the wavelet function, and the layer is set to 10 when considering the sampling frequency of the signals. The obtained 10th-lever approximate content is considered the baseline drift of a signal.

The programs (Marwan, 2002) used for recurrence quantification analysis (RQA) in the current study consume a large amount of memory and time with increasing in the length of the signals for each window which are sent for analysis. Therefore, resampling the signals is a more viable option than increasing the window size to guarantee adequate periods of pulse signals for each analyzed window. In the current work, all pulse signals are resampled to decrease the sampling frequency from 720 to 360 Hz before being analyzed for RQA. The layer of wavelet is set at 9 to obtain the ninth-lever approximate contents for baseline drifting for WRQA because of the changing sample frequency of the signals.

Methods

The nonlinear time-series analysis is based on the reconstruction of the phase space, which is derived from the embedding theory proposed by Takens (Takens, 1985). For a given time series $\{u_n | n = 1, 2 \ldots N\}$, where N is the length of the time series, the phase space trajectories x_i can be reconstructed using an embedding dimension m and a time delay τ.

$$x_i = \left(u_i, u_{i+\tau}, \cdots, u_{i+(m-1)\tau}\right), i = 1, 2, \cdots, M, x_i \in R^m \quad \ldots(1)$$

where M equals N-(m-1)τ.

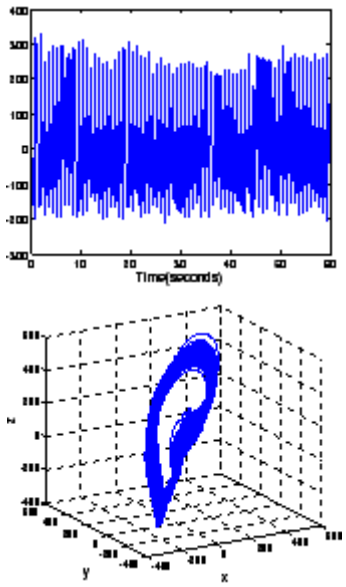

Fig. 1. Typical normal pulse time series sample illustrating the reconstruction, where $y=x+\tau$, $z=x+2*\tau$. (m=3, τ=5)

Sample entropy and multiscale entropy

The time series should be reconstructed when the delay τ is set as 1 in the sample entropy (SampEn) analysis. In SampEn, the distance between x_i and x_j, where i is not equal to j (i=1,2,……M; j=1,2,……M), is calculated based on the following equation:

$$d(x_i, x_j) = \max\left\{\left|u_{(i+k)} - u_{(j+k)}\right|, 0 \le k \le m-1\right\} \quad i \ne j \quad \ldots(2)$$

And r is introduced as the threshold for calculating $n_i(m, r)$ which is the number of vectors that satisfy $d(x_i, x_j)$d" r. Therefore, $C_i(m, r)$ can be defined as follows:

$$C_i(m,r) = n_i(m,r)/M \quad \ldots(3)$$

Let $C(m, r)$ represent the average of $C_i(m, r)$.

$$C(m,r) = 1/M\sum_{i=1}^{M} C_i(m,r) \quad \ldots(4)$$

Then the embedding dimension m should be replaced by m+1. The above mentioned step can be used to compute $C(m+1, r)$. Now, SampEn can be described as follows:

$$SampEn(m,r,N) = -\ln\left(C(m+1,r)/C(m,r)\right) \ldots(5)$$

According to previous studies (Pincus, *et al*., 1994), $m = 2$ and $r = 0.15$*standard deviation are proper for a given time series.

Multiscale entropy (MSE), which was developed based on SampEn, was introduced by Costa *et al.* (Costa, *et al.*, 2003). Before the time series is sent for calculation using SampEn, it should first be constructed as a coarse-grained time series using a scale factor.

$$y_j^{(s)} = \frac{1}{s}\sum_{i=(j-1)s+1}^{js} x_i, 1 \le j \le N/s \quad ...(6)$$

where *s* is the scale factor, *x* is the raw time series (in the current paper, *x* is the preprocessed time series), and *y* is the coarse-grained time series. When *s* is equal to 1, *y* is the raw time series. In the present work, the biggest scale factor is set as 5 for MSE analysis.

Although the SampEn algorithm is suitable for shorter-term time series, the irregularity measure still becomes unstable if the length of the input data is too short. MSE is developed based on SampEn so estimating the minimum length of SampEn analysis with different sampling rates is necessary; the results are shown in Figure 2 (the SampEn values of a pulse signal and a sine signal, the mean period of which is 0.76 seconds, sampled at 720, 360, 240, 180, and 144 Hz, respectively, were calculated). Figure 2 shows that these SampEn values become stable when the lengths (N) of a pulse wave and a sine wave are greater than 1200 and 1000, 850 and 600, 750 and 500, 550 and 350, and 500 and 250, respectively, with different sample frequencies. Therefore, 2500 sampling points of pulse signals are selected in the current work for MSE analysis.

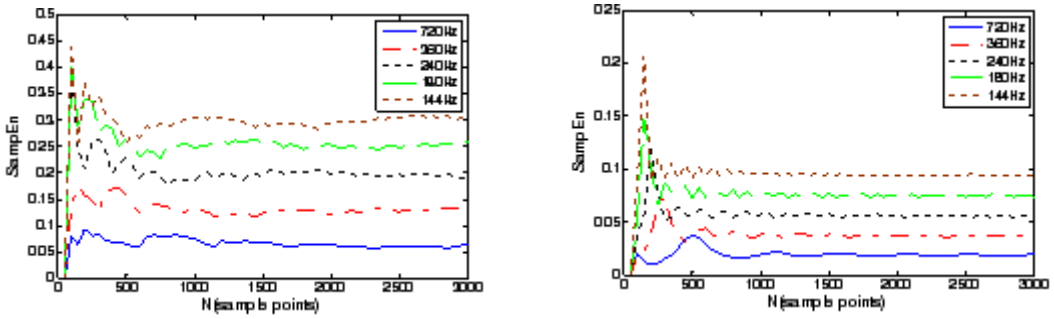

Fig. 2. Effect of length N on the value of SampEn (a. pulse wave; b. sine wave)

Recurrence plot (RP) and RQA

After the time series was reconstructed, the RP can be defined as follows:

$$R_{i,j} = H\left(e - \left\|x_i - x_j\right\|\right) \quad ...(7)$$

where e is the size of neighborhood, is the norm, and $H(x)$ is the Heaviside function.

RQA was introduced by Zbilut and Webber (Zbilut *et al.*, 2006) to extend quantitatively the method of RP. Marwan *et al.* (Marwan *et al.*, 2002) introduced additional measures of complexity based on RP, which can identify laminar states and their transitions to regular and chaotic regimes in complex systems. There are several common measures defined with the RP in RQA, such as the recurrence rate (RR), the percentage of recurrence points forming diagonal structures (DET), the percentage of recurrence points that form vertical structures (LAM), the average length of the diagonal structures (L), the Shannon entropy of the probability distribution of the diagonal line lengths (ENTR), trapping time (TT), the lengths of the longest diagonal line and longest vertical line (Lmax and Vmax), the mean recurrence time of the first type (T_1) and the mean recurrence time of the second type (T_2) (Gao, 1999).

RESULTS AND DISCUSSION

WMSE analysis

To detect the changes in morphology of a pulse signal, WMSE is proposed for the analysis of wrist pulses. A pulse signal is analyzed using a moving window with a size of 2500 sampling points and each time the window moves forward by 500 sampling points, as illustrated in Figure 3. For each window, the MSE measures are calculated using 5 as the biggest scale factor. Therefore, several irregularity measure values will be obtained from one scale factor. Then the mean value (MWMSE)

and the standard deviation (SWMSE) of the irregularity measure values will be computed as the variables to distinguish the three kinds of pulse signals. The mathematical expressions for MWMSE and SWMSE are shown as follows:

$$MWMSE_s = \frac{1}{NW}\sum_{i=1}^{NW} MSE_i^s \quad ...(8)$$

$$SWMSE_s = \sqrt{\frac{1}{NW}\sum_{i=1}^{NW}\left(MSE_i^s - MWMSE\right)^2} \quad ...(9)$$

where NW is the number of windows, and MSE_i^s is the value of MSE calculated in the i-th window on scale s.

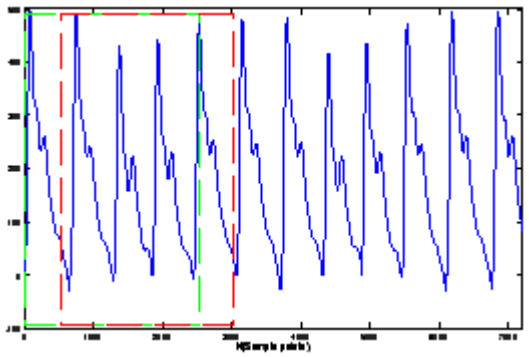

Fig. 3. Schematic illustration of the method for determining the size of the window and the length of each movement of the window with 2500 sample points of pulse signals. The sample points in the green window will be sent for calculating MSE first, and those in the red window will be calculated next

Considering all mean values of MWMSE on different scale factors, there were no obvious differences between the normal and slippery groups, as shown in Figure 4(a). Similar to the findings on MWMSE, the differences in SWMSE between the normal and slippery groups were not obvious. However, the differences between the wiry group and the two other groups are much clearer, as shown in Figure 4(b). This finding was proven using analysis of statistical independence (the p values of the SWMEs of the normal and slippery groups are all higher than 0.05, and those of the wiry group and the two other groups are all less than 0.001).

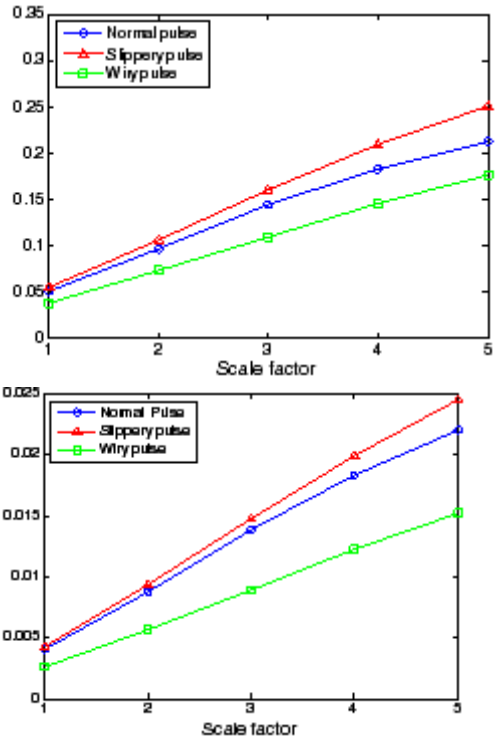

Fig. 4. Windowed MSE analysis of a pulse signal. Panel a shows the mean value of MWMSE of all the samples in each group, in which there is a sustained increase in complexity with an increase in scale of all three groups. In panel b, the mean values of SWMSE of all the samples in each group are shown

WRQA

A pulse signal is analyzed by using WRQA with a moving window that has a size of 1000 sampling points and each time the window moves forward by 300 sampling points in order to detect the changes in morphology of a pulse signal. Therefore, there are at least two periods of each pulse signal in each analyzed window, and for most of the subjects, there would be more than three periods in each window at the current sample frequency. For each window, the measures of RQA (RQAs) are calculated using an embedding dimension (m) of 3, a delay ($\hat{o}$) of 5, and minimal lengths of both diagonal and vertical structures of 2. According to Ref. (Marwan, 2002), the size of neighborhood (e) should be held constant to keep RR (one of measures of RQA) at approximately 10%. The value of e is then increased until other measures of RQA become stable.

On the other hand, Ref. (Zbilut, *et al*., 2006) indicated that one guideline for selecting a proper e is to keep the RR low from 0.1% to 2.0%. The measures of WRQA are computed using different values of e to keep the RR in the range of 1% to 12%. Finally, a value of 0.2*standard deviation of the resampled pulse signal for e is suitable for the signals used in the current study. For each subject, the mean value (MWRQAs) and standard deviation (SWRQAs) of the measures of WRQA are calculated based on each window as the variables to distinguish the three kinds of common TCM pulse signals which will be described in detail in Section 4. The mathematical expressions for MWRQAs and SWRQAs are provided as follows:

$$MWRQAs_j = \frac{1}{NW}\sum_{i=1}^{NW} RQA_i^j \qquad (10)$$

$$SWRQAs_j = \sqrt{\frac{1}{NW}\sum_{i=1}^{NW}\left(RQA_i^j - MWRQA\right)^2} \qquad (11)$$

where NW is the number of windows, and RQA_i^j is the value of the j-th RQAs calculated in the i-th window.

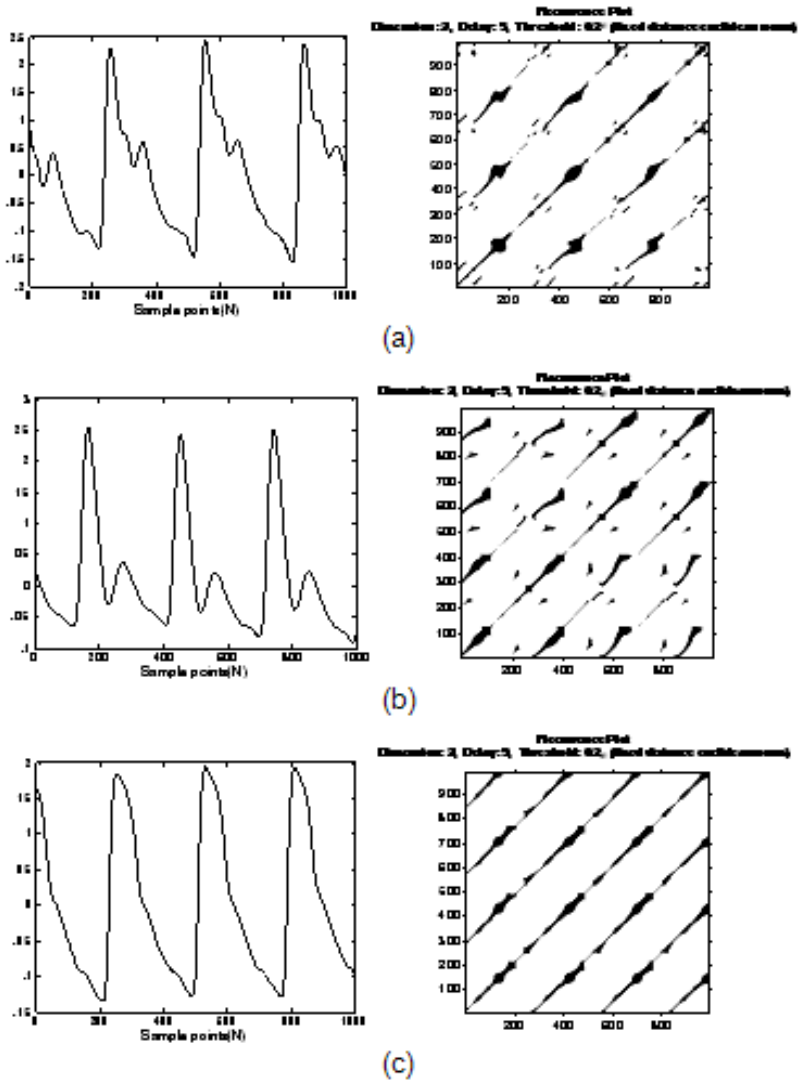

Fig. 5. Typical TCM pulse signals and their RPs with m=3, $\hat{o}$=5, and e=0.2*standard deviation (a. normal pulse signal, b. slippery pulse signal, and c. wiry pulse signal)

Figure 5 shows the typical TCM pulse signals and their RP. Table 1 shows that in the first seven measures and the last measure of MWRQAs, the mean values of them from the wiry group are the highest among all groups. Meanwhile, the mean values of RR, DET, and Vmax in the normal group are the lowest, whereas the other measures of MWRQAs, except for T_1, in the slippery group are the lowest. The analysis of statistical independence denotes that the differences between the wiry group and the two other groups of pulse signals are much more significant than those between the normal and slippery groups, whether in terms of MWRQAs or SWRQAs. This finding agrees with the result of WMSE described previously. However, for some measures such as L, LAM, and T_2 of MWRQAs and T_1 of SWRQAs, some obvious differences can still be observed between the normal and slippery groups of pulse signals shown in Table 1.

Table 1. Result of WRQA for the three kinds of TCM pulse signals

RQA	MWRQAs			SWRQAs		
	Normal group	Slippery group	Wiry group	Normal group	Slippery group	Wiry group
RR	0.064±0.007	0.066±0.015$^{\#\#}$	0.076±0.010$^{\wedge\wedge}$	0.007±0.002*	0.009±0.004	0.008±0.003
DET	0.9978±0.0010	0.9979±0.0008$^{\#\#}$	0.9986±0.0005$^{\wedge\wedge}$	0.0005±0.0003	0.0004±0.0002$^{\#\#}$	0.0003±0.0002$^{\wedge\wedge}$
L	29.212±4.412*	27.392±5.881$^{\#\#}$	39.425±8.294$^{\wedge\wedge}$	3.470±0.815	3.529±1.565$^{\#}$	4.761±1.880$^{\wedge\wedge}$
L_{max}	304.367±27.306	304.500±55.863$^{\#\#}$	558.417±260.414$^{\wedge\wedge}$	37.613±19.915*	57.852±38.104$^{\#}$	117.019±93.081$^{\wedge\wedge}$
ENTR	4.090±0.135	4.038±0.211$^{\#\#}$	4.342±0.175$^{\wedge\wedge}$	0.121±0.030	0.133±0.056	0.117±0.032
LAM	0.996±0.001**	0.994±0.003$^{\#\#}$	0.997±0.001$^{\wedge\wedge}$	0.0010±0.0004**	0.0017±0.0008$^{\#\#}$	0.0007±0.0003$^{\wedge\wedge}$
TT	14.874±1.737*	13.741±3.925$^{\#\#}$	17.838±3.087$^{\wedge\wedge}$	1.428±0.453	1.848±0.950	1.711±0.735
V_{max}	59.373±6.757	65.106±19.818	63.429±15.032	7.057±3.467*	8.643±4.221	10.628±6.527$^{\wedge}$
T_1	11.134±1.002	11.974±2.935$^{\#\#}$	9.879±1.237$^{\wedge\wedge}$	1.038±0.318**	1.452±0.457$^{\#\#}$	0.931±0.259
T_2	191.438±12.477**	170.313±14.558$^{\#\#}$	203.792±19.328$^{\wedge\wedge}$	9.383±2.645*	8.545±3.424$^{\#}$	6.553±2.813$^{\wedge\wedge}$

Note: Nonparametric Mann–Whitney U test: p represents significance; * is for $p<0.05$ and ** is for $p<0.01$ between the normal and slippery groups; ^ is for $p<0.05$ and ^^ is for $p<0.01$ between the normal and wiry groups; and # is for $p<0.05$ and ## is for $p<0.01$ between the slippery and wiry groups.

Table 2. Classification results using SVM

Experiment	Sample class	Testing samples	Accuracy (%) (WMSE)	(WRQA) Average accuracy	Accuracy (%) (WMSE&WRQA)	Average accuracy	Accuracy (%)	Average accuracy
No. 1	Normal VS	48	75.33	79.30	85.33	87.68	84.89	89.47
	Slippery	48	82.67		89.78		93.56	
No. 2	Normal VS	48	94.00	91.73	94.00	88.57	93.78	90.68
	Wiry	48	89.56		83.33		87.56	
No. 3	Slippery	48	80.67	83.13	95.78	96.84	93.78	90.58
	VS Wiry	48	85.56		97.78		87.78	
All three groups								
No. 4	Normal,	48	83.11	77.77	81.33	84.70	81.33	86.15
	Slippery	48	64.67		89.56		89.56	
	and Wiry	48	85.78		83.56		85.78	
	group							

Note: The definition of accuracy is expressed as follows: Accuracy= number of samples classified correctly in one class/ the total number of samples in the class*100%.

Classification by support vector machine (SVM)

An SVM (Chang, *et al*., 2001) (using five-fold cross-validation and RBF kernel function) is used to classify the variables obtained through WMSE and WRQA. The result is shown in Table 2. An accuracy of 87.68% is achieved when distinguishing the normal and slippery groups using WRQA, and the accuracy reaches 89.47% using both WMSE and WRQA. The average accuracy of the normal and wiry groups is 91.73% using WMSE, which indicates that 12 of the 96 samples are misclassified. The average accuracy reaches 96.84% in the slippery and wiry groups using WRQA, which indicates that only 3 of the 96 samples are misclassified. By mixing all three groups together, the accuracy of the classification can reach 84.70% using WRQA and 86.15% using both WMSE and WRQA, which is encouraging.

DISCUSSION

In TCM theory, a normal pulse reflects a healthy body condition, which in turn indicates the normal function of the heart and blood vessels. The main characteristics of a normal pulse are a pulse rate that is neither fast nor slow, the position needed to feel the pulse that is neither superficial nor deep, and a pulse intensity that is neither strong nor weak. A normal pulse is always detected from the youth.

A slippery pulse comes and goes smoothly and when felt by a doctor, it resembles beads rolling under the finger. Based on clinical observations, a cardiovascular system detected as a slippery pulse has low peripheral resistance, good compliance of blood vessels, and sufficient stroke volume, indicating the good functioning of the heart and blood vessels. A slippery pulse is always detected from the youth, athletes, and pregnant women. However, a person who suffers from ailments such as cough with sputum and fever can also have a slippery pulse.

Contrary to the condition of the blood vessels represented by a slippery pulse, a wiry pulse is always related to high peripheral resistance and bad compliance of blood vessels. Feeling a wiry pulse is like palpating the string of a musical instrument. The pulse is long and straight and is common in old people. Sometimes, detecting a wiry pulse in old people does not necessarily indicate an unhealthy condition. Actually, a wiry pulse means that the body condition is not as good as that of a young individual. However, a wiry pulse can also represent problems of the liver and gallbladder, pain, phlegm retention, malaria, or consumptive diseases.

MSE measures the degree of self-similarity of the time series with different scales. If the values of MSE increase with an increase in scales, the observational time series is irregular and vice versa. The result of WMSE in the current paper shows that all the time series sent for analysis are irregular, as shown in Figure 4(a). This kind of increase with an increase in scales may be attributed to the loss of correlation between the two nearest points sent to be analyzed with an increase in scales.

In Ref. (Costa *et al*., 2005), the MSE method indicates that healthy systems are more complex than systems with illnesses, which reflects the capability of healthy systems to adapt and function in an ever-changing environment. This finding agrees with the obtained results from WMSE analysis when those of SWMSE are considered. The higher values of MWMSE and the mean value of MWMSE in the slippery group seem to indicate that the cardiovascular system represented by a slippery pulse is more complex than that represented by a normal pulse. However, the higher values of SWMSE in the slippery group, especially with an increase in scale, indicate that the complexity (irregularity) varies within different segments of the same signal. This finding means that the slightly higher MWMSE values in the slippery group cannot represent the higher degree of complexity of the entire signal but only of some segments within the signal. This kind of instability may be attributed to some pathological changes in the cardiovascular system of the patient who has a slippery pulse.

Because the patients who have slippery pulse are always suffering from ailments, which means their cardiovascular system don't damage severe or permanently, it is not strange that the results of WMSE from normal pulse signals are similar with that from slippery pulse signals. A wiry pulse is always related to a deteriorating function of the cardiovascular system, so the low value of WMSE may be attributed to the loss of complexity in the system.

RQA focuses mainly on the diagonal and vertical structures of RP. Based on Ref. (Zbilut *et al*., 2006), periodic signals will display very long diagonal lines in RPs, chaotic signals will display short diagonal lines, and stochastic signals will display no diagonal lines, so as to the vertical structures.

The RR in RQA represents the percentage of recurrent points falling within the specified size of the neighborhood. The value of RR will be lower when calculated using an irregular signal than when computed using a periodic signal with the same size of neighborhood. This result is due to the low correlation between the two nearest points of an irregular signal. Moreover, the value of RR will be significantly low when the analyzed signal is a stochastic signal. This outcome is due to the difficult estimation of the relationship between the two nearest points of a random signal (same size of neighborhood).

The L in RQA is described as the average length of the diagonal lines on RP. Generally, a shorter L results in a more chaotic (less stable) signal. LAM in RQA measures the proportion of recurrent points, which can form vertical line structures. Similar to the two measures of RQA described previously, LAM can detect the degree of chaos of a signal. A periodic signal will result in a high proportion of LAM, whereas a chaotic signal will result in a low proportion of LAM. The value of LAM will be zero if the analyzed signal has random numbers (with same proper size of neighborhood).

Considering the different groups of pulse signals when interpreting the value of these three RQA measures, the higher mean value from the wiry group indicates a greater regularity in its signals. However, the differences between the normal and slippery groups are still not distinguishable, similar to those of the MSE analysis described previously.

The recurrence time of a finite trajectory is described generally as the amount of time needed to re-traverse a trajectory. As reported in Ref. (Gao,*et al*.,2000), the mean recurrence time of the first type (T_1) and the second type (T_2) is related to the information dimension of the attractor using simple scaling laws. In the obtained result (Table 1), the significant differences between the normal and slippery groups of T_2 in MWRQAs and T_1 in SWRQAs can help in distinguishing these two groups of TCM pulse signals better. The differences can mitigate the fact that there are no significant differences observed between these two groups in terms of other features in the current research. Moreover, based on Table 1, most measures of SWRQAs in the slippery group show higher values than those of the two other groups, which denote some instability among different segments of a slippery pulse signal. This finding is similar to the result of SWMSE, so this kind of instability may be a property of slippery pulse signals.

Table 2 shows the high level of accuracy in the classification of the three kinds of TCM pulse signals. This finding indicates that WMSE analysis and WRQA, both of which consider the effect of changes in the morphology of a pulse signal, may be useful for distinguishing the three common kinds of pulses defined in TCM and thereby benefit pulse diagnosis.

CONCLUSION

The cardiovascular system is a complex system, and the wrist pulse, which reflects the changes in this system, is the main diagnostic evidence in pulse diagnosis in TCM, similar to ECG, ABP, and HRV. Linear methods exclude the nonlinear properties present in pulse signals and interval variability analysis ignore the change in the morphology of a pulse signal, so WMSE and WRQA are used to analyze pulse signals in the current paper.

The results from the current study reveal clearly that when the cardiovascular system is represented by a wiry pulse, there is a loss of complexity in the results of WMSE and WRQA compared with the results from other kinds of pulse signals. Although the differences in the analyzed results between the normal and slippery pulse signals are not as significant as those between the wiry pulse signals and the two other groups, normal pulse signals are found to be slightly more stable than slippery signals based on SWMSE and SWRQA.

The recurrence time, especially T_2, can also distinguish normal from slippery pulse signals well. Finally, the high level of accuracy in the classification indicates that the analysis of pulse

signals using WMSE and WRQA, both of which consider the effect of changes in the morphology of a pulse signal, is appropriate and can be useful for distinguishing the three common kinds of pulses defined in TCM, thereby benefitting pulse diagnosis.

ACKNOWLEDGMENTS

This work was supported by National Natural Science Foundation of China (No. 81270050, 30901897, 81173199 and 30701072), and Innovation Program of Shanghai Municipal Education Commission (Grant No.11YZ71).

REFERENCES

1. Bär KJ, Schulz S, Koschke M, Harzendorf C, Gayde S, Berg W, Voss A, Yeragani VK., Boettger MK., Correlations between the autonomic modulation of heart rate, blood pressure and the pupillary light reflex in healthy subjects. *Journal of the Neurological Sciences,* 2009; **279**(1-2): 9–13
2. Casaleggio A, Braiotta S., Estimation of Lyapunov Exponents of ECG Time Series - The Influence of Parameters. Chaos, *Solitons and Fractals*, 1997; **8**(10): 1591-1599
3. Chang CC, Lin CJ., "LIBSVM: a library for support vector machines", http:// www.csie.ntu.edu.tw/~cjlin/libsvm/index.html Accessed 24 May 2011, 2001.
4. Chen YH, Zhang L, Zhang D, Zhang DY., Wrist pulse signal diagnosis using modified Gaussian models and Fuzzy C-Means classification. *Medical Engineering and Physics*, 2009; **31**(10): 1283-1289.
5. Chesnokov YV., Complexity and spectral analysis of the heart rate variability dynamics for distant prediction of paroxysmal atrial fibrillation with artificial intelligence methods. *Artificial Intelligence in Medicine*, 2008; **43**(2): 151-165
6. Costa M, Goldberger AL, Peng CK., Multiscale entropy analysis of biological signals. *Physical review E*, 2005; **71**: 1-18
7. Costa M, Peng CK, Goldberger AL, Hausdorff JM., Multiscale entropy analysis of human gait dynamics. *Physica A*, 2003; **330**: 53-60
8. Crilly M, Coch C, Bruce M, Clark H, Williams D., Indices of cardiovalscular function derived from peripheral pulse wave analysis using radial applanation tonometry: a measurement repeatability study. *Vascular medicine*, 2007; **12**(3): 189-197
9. Fei ZF., Study of pulse diagnosis in Tradition Chinese Medicine. The Press of Shanghai University of Traditional Chinese Medicine, Shanghai (in Chinese), 1991.
10. Gao JB., Recurrence time statistics for chaotic systems and their applications. *Physical Review Letters,* 1999; **83**(16):3178-3182
11. Gao JB, Cai HQ., On the structures and quantification of recurrence plots. *Physics Letter A*, 2000; **270**(1-2): 75-87
12. Javorka M, Trunkvalterova Z, Tonhajzerova I, Javorkova J, Javorka K, Baumert M., Short-term heart rate complexity is reduced in patients with type1 diabetes mellitus. *Clinical Neurophysiology*, 2008; **119**(5): 1071-1081
13. Jokinen V, Syvanne M, Makikallio TH, Airaksinen KEJ, Huikuri HV., Temporal age-related changes in spectral, fractal and complexity characteristics of heart rate variability. *Clinical Physiology,* 2001; **21**(3):273–81
14. Lee CT, Ling YW., Spectrum analysis of human pulse. IEEE Tran. *On BME,* 1983; **30**: 348-352
15. Marwan N., Commandline Recurrence Plots, 2002.
16. http://www.agnld.uni-potsdam.de/~marwan/ toolbox/ Accessed 24 May 2011.
17. Marwan N, Wessel N, Udo M, Schirdewan A, Kurths J., Recurrence-plot-based measures of complexity and their application to heart-rate-variability data. *Physical Review* E, 2002; **66**(2): 026702
18. Perakakis P, Taylor M, Martinez-Nieto E, Revithi L, Vila J., Breathing frequency bias in fractal analysis of heart rate variability. *Biological Psychology*, 2009; **82**(1): 82-88.
19. Persson PB., Chaos in the cardiovascular system: An update. *Cardiovascular Research,* 1998; **40**(2): 257-264
20. Pincus SM, Goldberger AI., Physiological time-series analysis: what does regularity quantify? *Am J Physiol: Heart Circ Physiol,* 1994; **266**(4): 1643-1656
21. Qian W., Feature extraction of pulse wave by using Gaussian function. *Chinese journal of biomedical engineering*, 1994; **13**(1): 1-7 (in Chinese)
22. Song JQ, Dong YW, Wu SJ., Application of cepstral techniques to analyzing pulse signals. *Journal of Shanxi Normal University (Natural Science Edition*), 1997; **25**(2): 35-39 (in Chinese)
23. Takens F., On the numerical determination of the dimension of an attractor. Lecture Notes in Mathematics, 1985; **1125**: 99-106
24. Wang B, Luo J, Xiang J, Yang Y., Power spectral

analysis of human pulse and study of traditional Chinese medicine pulse-diagnosis mechanism. *Journal of Northwestern University (Natural Science Edition*), 2001; **31**(1): 22-25 (in Chinese)

25. Wessel N, Ziehmann C, Kurths J, Udo M, Schirdewan A, Voss A., Short-term forecasting of life-threatening cardiac arrhythmias based on symbolic dynamics and finite-time growth rates. Physical review E, 2000; **61**(1):733-739
26. Wu LN, Liu SQ, Wang LL., Realization of pulse wave detecting system with time-domain signal processing method. Transducer and Microsystem Technologies 2008; **27**(9):72-74 (in Chinese)
27. Xie JY, Cai KB, Wang YD., Application of Continuous Wavelet Transform to Pulse Signal Processing. *Journal of Chongqing University,* 2003; **26**(1): 66-68,76 (in Chinese)
28. Xu LS, Meng MQH, Qi XH, Wang KQ., Morphology variability analysis of wrist pulse waveform for assessment of arteriosclerosis status. *J Med Syst,* 2010; **34**(3):331-339
29. Zbilut JP and Webber CL., Recurrence Quantification Analysis. *Wiley Encyclopedia of Biomedical Engineering,* 2006.
30. Zhang DY, Zhang L, Zhang D, Zheng YP., Wavelet based analysis of Doppler ultrasonic wrist-pulse signals. In: Proceedings of the ICBBE 2008 conference, 2008; **2**: 539–543
31. Peña MA, Echeverría JC, García MT, González-Camarena R., Applying fractal analysis to short sets of heart rate variability data. *Med Biol Eng Comput*, 2009; **47**(7): 709-717.